Electrokinetic dewatering of phosphatic clay settling areas: numerical simulation and economic assessment

J.P. McKinney and M.E. Orazem
Department of Chemical Engineering, University of Florida, Gainesville, FL

Abstract

A mathematical model is presented for the electrokinetic dewatering of suspensions of phosphatic clays. The modeling approach couples a boundary-element model for solution of Laplace's equation to a recently developed constitutive equation that relates the change in solids content with applied electric field and time. The observation that the electric field controls both the maximum solids content achievable and the time required to reach that value is shown to severely constrain the application of electrokinetic dewatering strategies to an entire clay settling area. The approach, however, may be feasible for implementation as part of a continuous plant process.

Key words: CP_3D, Simulations, Electrokinetics, Dewatering, Clays, Clay settling areas (CSAs)

Introduction

Electrokinetic dewatering, which does not require the addition of adulterants that could interfere with future recovery of residual phosphate ore, may be an attractive method to enhance solid-liquid separation of phosphatic clay suspensions associated with the phosphate mining industry. The suspensions, containing roughly 10 wt% solids, are held in large impoundments called clay settling areas (CSAs) (Carrier, 2001). The CSAs cover an area of over 388 km^2 (150 sq mi) in central Florida, representing 30% of the land that has been mined (Barnett, 2008). The need to reduce both the land area dedicated to storage of phosphatic clay suspensions and the water consumed in the mining operation has motivated a search for methods that will increase the solids content in the CSAs and release clean water.

Electrokinetic dewatering has been demonstrated for clay suspensions and other mine tailings (Shang and Lo, 1997; Ho and Chen, 2001; Fourie et al., 2007). McKinney and Orazem (2011) report on electrokinetic dewatering of clay slurries obtained from the Four Corners phosphate mine located in central Florida, owned and operated by Mosaic Fertilizer, LLC. They observed that the separation process consisted of a short-time behavior, in which the increase in solids content was proportional to the product of the electric field and the time over which the field was applied, and a long-time behavior, in which a maximum solids content was reached. This maximum and the time required to achieve this limiting value were strong functions of the electric field. A constitutive relationship was developed to characterize the electrokinetic dewatering, providing the change in solids content of the clays in terms of electric field and operating time.

The object of this work was to use the constitutive relationship to estimate the power requirements for the application of electrokinetic dewatering to a large-scale CSA.

Approach

CP_3D, a mathematical model developed to simulate cathodic protection of buried pipelines (Riemer and Orazem, 2005b; Riemer, 2000), was used to model the dewatering of a CSA. The resistivity of the clay suspensions was assumed to be both uniform and constant and pH variations associated with electrochemical reactions were ignored.

Constitutive relation. The constitutive relation for solids content as a function of operating time and applied electric field takes the form (McKinney, 2010; McKinney and Orazem, 2011)

$$\Delta w_c = [(0.77tE)^{-n} + (7.1 \log_{10}(E) + 16.5)^{-n}]^{-1/n} \qquad (1)$$

where $n=5$ is a dimensionless parameter that controls the transition from short-time to long-time behavior, E has units of V/cm and t has units of hours. The change in solids content Δw_c is referenced to the initial composition, which was generally between 9 and 11 wt% solids. The predicted increase in solids content is presented in Fig. 1 as a function of time, with the applied electric field as a parameter. Equation (1) was used to assess the final solids content associated with a given electric field and the time required to reach that value.

Solution of Laplace's equation. The electric field in the CSA was calculated using the computer program CP_3D (Riemer and Orazem, 2005b; Riemer, 2000). The passage of current through the suspension is governed by Laplace's equation:

Paper number MMP-10-040. Original manuscript submitted August 2010. Revised manuscript accepted for publication November 2010. Discussion of this peer-reviewed and approved paper is invited and must be submitted to SME Publications Dept. prior to November 30, 2011.

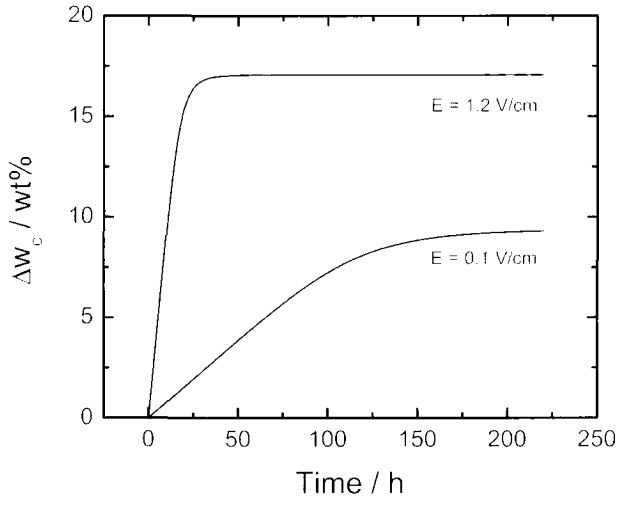

Figure 1 — The change in solids content predicted by the constitutive relationship taken from McKinney and Orazem (2011) and given as Eq. (1). The results are presented as a function of time with applied electric field as a parameter.

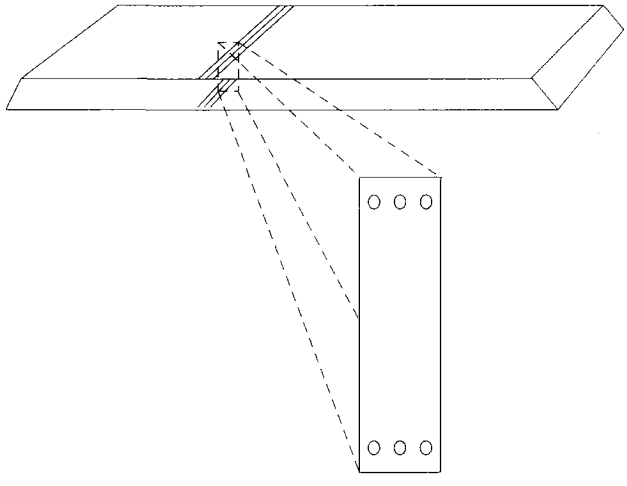

Figure 2 — Representation of a large CSA with one-mile-long horizontal cylindrical electrodes spaced equally along top and bottom surfaces. The detail represents a cross-section of the cylindrical electrodes. Although only rows of three cylinders are shown, the simulation was scaled for rows that extend to a distance of one mile.

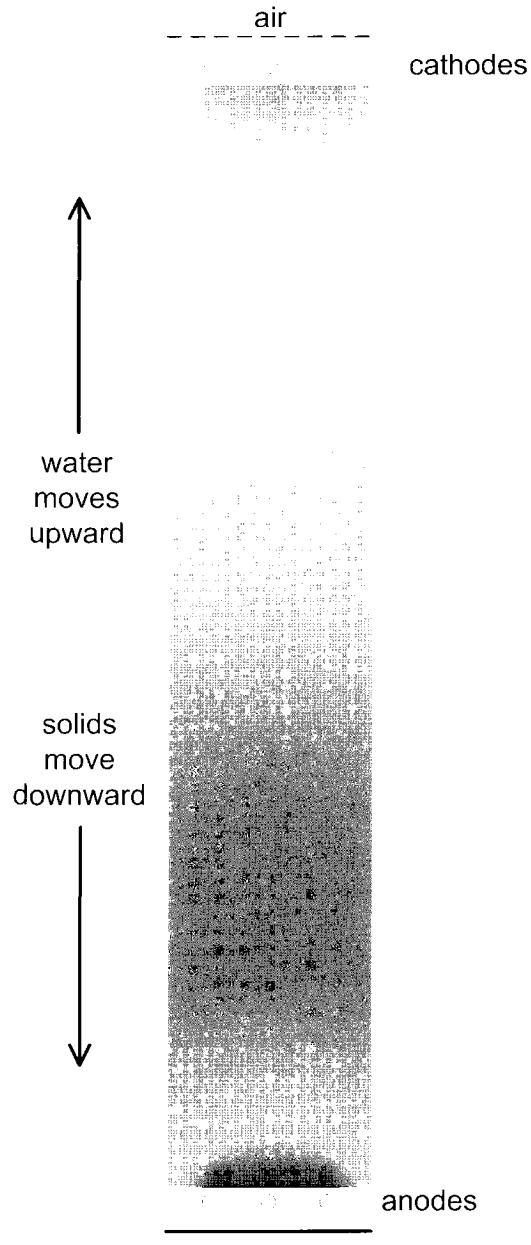

Figure 3 — Illustration of horizontally oriented electrode configuration presented in Fig. 2 with the calculated potential distribution from CP_3D presented as a false-color image.

$$\nabla^2\Phi = 0 \qquad (2)$$

which was solved using the boundary element method (BEM). The formulation of the boundary element method used in this study can be found elsewhere (Riemer and Orazem, 2005b; Brebbia and Walker, 1980; Stakgold, 1979; Telles et al., 1985; Aoki and Kishimoto, 1990). The program has been applied to model cathodic protection of pipelines with coating flaws (Riemer and Orazem, 2005b), to analyze the cathodic protection of tank bottoms (Riemer and Orazem, 2005a), to predict effectiveness of coupons for assessing cathodic protection of buried structures (Riemer and Orazem, 2000) and to assess the use of electrical potential survey data to assess the condition of buried pipes (McKinney et al., 2006; Moghissi et al., 2009).

The electrodes were modeled as cylinders of finite electrical conductivity and the model accounted for the associated attenuation of current through the length of the electrodes. The boundary condition accounted for oxygen generation at the anode and for oxygen reduction and hydrogen evolution at the cathode. A detailed description of the nonlinear kinetic expressions was presented by Riemer and Orazem (2005b). The reflection properties of Green's functions (Brebbia and Walker, 1980; Stakgold, 1979; Hartmann et al., 1985; Gray and Paulino, 1997) were used to create an insulating barrier at the suspension-air interface and at the bottom of the CSA. The model allows calculation of potential at arbitrarily chosen locations within the suspension or at the suspension-air surface.

CSA geometries. The tailings impounded in the CSA were assumed to have an initial 10 wt% solids content. The dimensions of the CSA were assumed to be 1.6 km (1 mi) wide, 1.6 km (1 mi) long and 12.2 m (40 ft) deep. Two different electrode

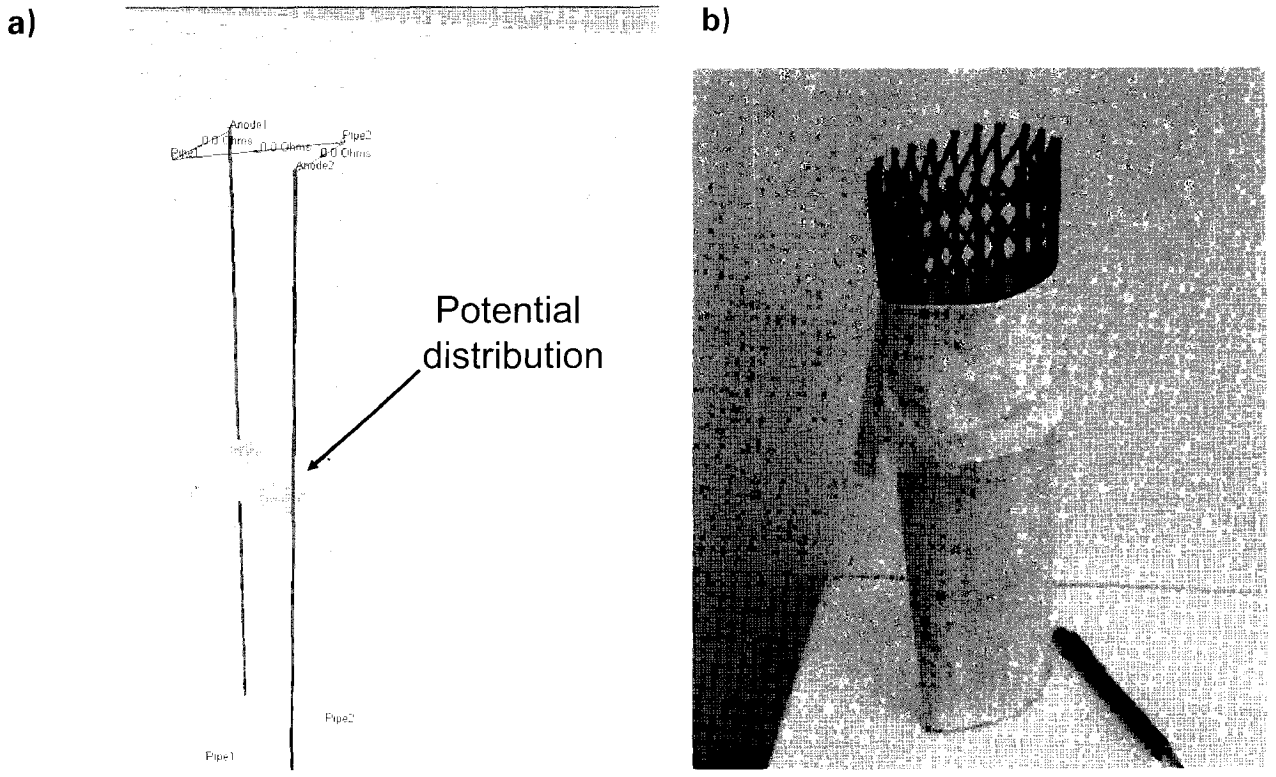

Figure 4 — Representation of a large CSA with vertically oriented cylindrical electrodes: a) unit cell of vertically oriented electrodes with a false-color image of the calculated potential distribution; and b) photograph of a geosynthetic electrode covered with a filter cloth required as a separator for removal of water using a vertically oriented cathode (taken from Fourie et al., 2007, copyright © 2008 NRC Canada or its licensors and reproduced with permission).

configurations were explored.

Horizontal electrode configuration. A schematic illustration of a CSA with a horizontal electrode configuration is given in Fig. 2. For the simulations presented here, cylindrical cathodes were placed near the surface of the simulated CSA and cylindrical anodes were placed near the bottom. The cylindrical electrodes were assumed to be 15.2 cm (6 in.) in diameter and placed 1.8 m (6 ft) apart. The electrode centerlines were placed 0.305 m (1 ft) below the air/CSA interface and 0.305 m (1 ft) above the CSA bottom, yielding a 11.6 m (38 ft) spacing between the electrode centerlines. The electrodes were 1.6 km (1 mi) long, consistent with a 2.56 km^2 (1 sq mi) CSA. They were assumed to be spaced equally along the entire CSA width of 1.6 km (1 mi).

The calculated potential distribution is presented in Fig. 3. Due to the large aspect ratio corresponding to the value of the distance between electrodes scaled by the electrode spacing, the potential distribution is uniform in the majority of the domain.

Vertical electrode configuration. The second configuration explored, presented in Fig. 4, employed electrodes oriented vertically, with cathodes and anodes placed diagonally from one another. The electrodes were represented as 7.6 cm (3 in.) diameter cylinders, 12 m (39.5 ft) long. The electrodes were 3.05 m (10 ft) apart, with a 4.31 m (10$\sqrt{2}$ ft) diagonal spacing.

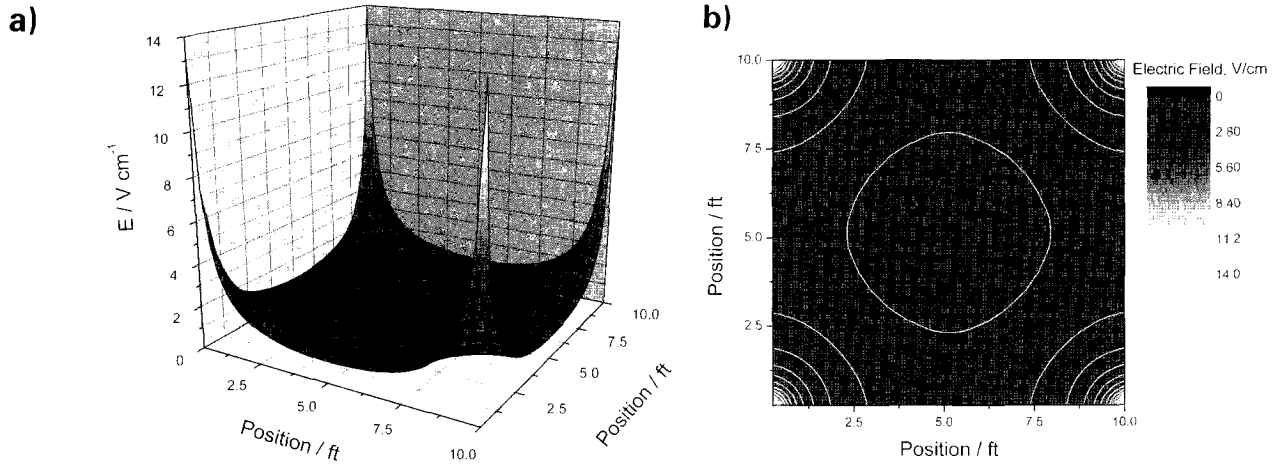

Figure 5 — Illustration of the electric field calculated from the simulation presented in Fig. 4a: a) three-dimensional representation and b) two-dimensional contour map.

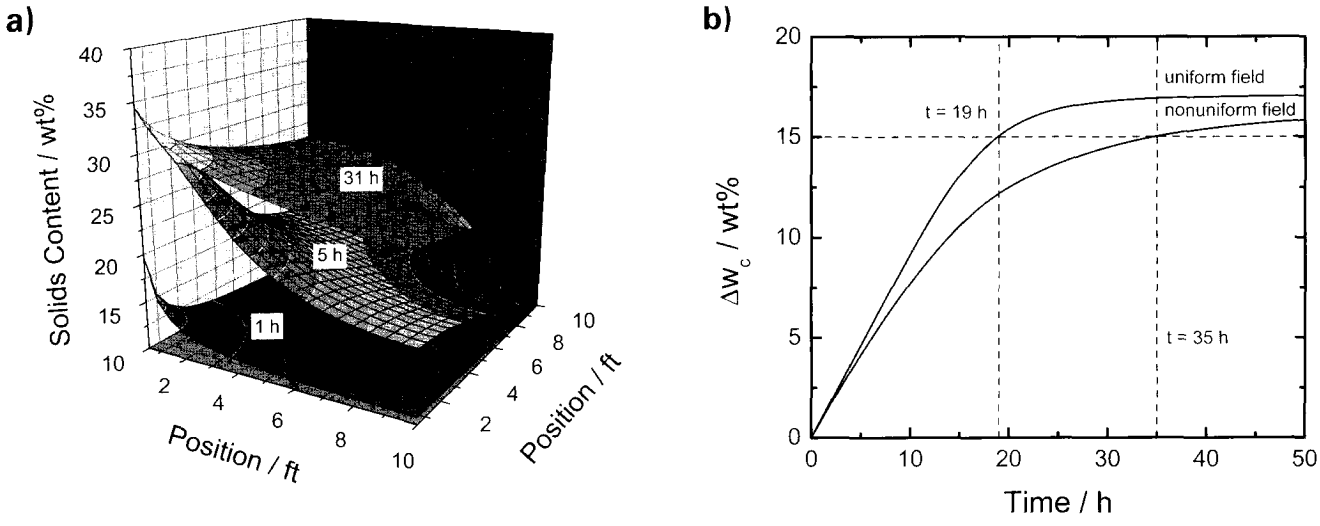

Figure 6 — Simulation results for a mean electric field of 1.2 V/cm: a) time-dependent solids content associated with the nonuniform electric field calculated for one quadrant of the geometry presented in Fig. 4a and b) the time required to reach a 15 wt% increase in average solids content for horizontal and vertical geometries.

The visualization in Fig. 4a represents a unit cell that is scaled up by adding additional electrodes to cover an entire square mile. A separator or filter cloth is required for vertically oriented cathodes to filter the clay from the water entering the inner diameter of the cathode. Such a system has been proposed by Fourie et al. (2007) (see Fig. 4b).

The electric field corresponding to the potential distribution shown in Fig. 4a is presented in Fig. 5. The location near the center where the electric field is flat represents a region where the field tends toward zero. The peaks shown at the corners represent areas where the electric field is much stronger. The experimental work, presented by McKinney and Orazem (McKinney, 2010; McKinney and Orazem, 2010), demonstrated a relationship between the solids content and the size of the electric field for a given elapsed time. Therefore, the nonuniform electric field should be expected to have nonuniform drying with locations in proximity of the electrodes (the four corners in Fig. 4a) having a strong change in solids content and the locations away from the electrodes (at the center in Fig. 4a) having significantly less change in solids content. The average electric field was calculated and the applied potential was adjusted such that the average electric field was the same for the horizontal and vertical configurations.

Results

Simulation results are presented in Table 1 for the electrokinetic dewatering of a full-scale CSA under an electric field of 1.2 V/cm. The elapsed time was chosen to allow the solids content to rise from 10 to 25 wt%. The simulations are compared to the experimental results utilizing a comparable electric field (McKinney, 2010; McKinney and Orazem, 2010). For the horizontal configuration, the time required to achieve the separation was taken directly from Eq. (1). To account for the nonuniform electric field, time-stepping simulations were performed for the vertical electrode configuration shown in Fig. 4a. Under the assumption that there was no lateral transport of water, profiles of solids content were generated as shown in Fig. 6a, in which the time-dependent solids content is pre-

Table 1 — Results of power and energy calculations for dewatering of simulated 2.6-km^2 (1-sq-mi) CSA. Solids content was increased from 10 to 25 wt%.

Configuration	Horizontal (Fig. 2)	Vertical (Fig. 4a)	Bench-top experiment (McKinney and Orazem, 2010)
Number of anodes	880	69,696	1
Number of cathodes	880	69,696	1
Electric field	1.2 V/cm	1.2 V/cm	1.1 V/cm
Time required	19 h	35 h	9 h
Cell potential	1,445 V	858 V	20 V
Current	34,617 A/electrode	586 A/electrode	0.04 A
Current required	4.09×10^7 A	3.05×10^7A	-
Power required	44,000 MW	35,000 MW	0.88 W
Energy required	8.4×10^8 kW h	1.2×10^9 kW h	7.9 W h
Water removed	2.02×10^{10} kg	2.02×10^{10} kg	0.57 kg
Energy requirement	41.3 W h/kg	60.7 W h/kg	13.9 W h/kg

sented for one quadrant of the geometry presented in Fig. 4a. The solids content is highest near the electrode and smallest in the center of the region between electrodes. The average solids content was calculated at each point in time. The results are presented in Figure 6b. As shown in Figure 6b, the time required to reach a 25 wt% solids content is larger for the geometry with a nonuniform electric field.

The most striking features of the results presented in Table 1 are the short time required to achieve the increase of solids content from 10 to 25 wt% and the enormous power requirement associated with this increase. The large power requirement can be attributed in part to the large separation between electrodes, resulting in a cell potential on the order of 1.4 kV. As the dominant potential drop is attributed to the Ohmic contribution of the clay suspension, the power is proportional to the square of the cell potential. The calculated energy requirement, however, is moderate. The values of 41.3 W h/kg water removed for a horizontal electrode configuration is in good agreement with the value of 13.9 W h/kg obtained over a shorter period of time in the bench-top experiments. A comparison of calculated and experimental energy requirements is presented in Fig. 7.

The power requirements are significantly reduced for a smaller electric field. Simulation results are presented in Table 2 for an applied electric field of 0.1 V/cm. As indicated by Eq. (1), the maximum solids content achievable by electrokinetic separation is lower for the smaller electric field. The simulations assume an increase in solids content from 10 to 18 wt%. The time required to achieve this separation is larger, i.e., 117 h for the horizontal configuration and 180 h for the vertical configuration.

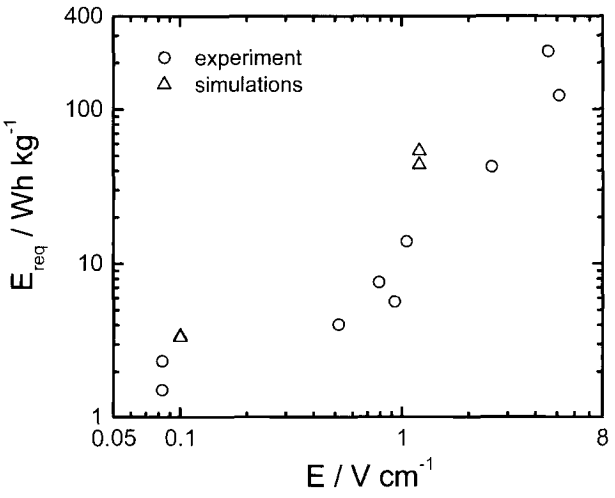

Figure 7 — Energy requirements for water removal as a function of the applied electric field. Experimental values taken from McKinney and Orazem (2011).

Economic implications

The power and energy requirements were estimated using a mathematical model in combination with the constitutive relationship. The power requirements for increasing the solids content of a 2.6-km^2 (1-sq-mi) CSA from 10 to 25 wt% were on the order of 40,000 MW. This requirement arose due to the short time over which the electric field was imposed. The energy requirement, however, is on the order of 10 x 10^8 kWh. At a cost of $0.10/kWh, the energy cost would be $80 million or $0.41/100 kg water removed.

The power requirement can be reduced by operating the electrokinetic dewatering process over a longer period of time. A consequence of the constitutive relationship given as Eq. (1) is that the electric field controls both the maximum solids content achievable and the time required to reach that value. Thus, the only way to increase the operating time is to process a portion of the CSA slurry using a semi-batch process. Such an operation would have the advantage that it could be optimized. For example, the gap between electrodes could be reduced; thereby reducing the cell voltage required to achieve a desired electric field. The time required to dewater the entire CSA would thus be increased.

While the economic analysis presented here does not account for capital and non-electrical operating costs, it is sufficient to illustrate the factors which would govern the implementation of electrokinetic dewatering methods in phosphate mining operations.

Table 2 — Results of power and energy calculations for dewatering of simulated 2.6-km^2 (1-sq-mi) CSA. Solids content was increased from 10 to 18 wt%.

Configuration	Horizontal (Fig. 2)	Vertical (Fig. 4a)	Bench-top experiment (McKinney and Orazem, 2010)
Number of anodes	880	69,696	1
Number of cathodes	880	69,696	1
Electric field	0.1 V/cm	0.1 V/cm	0.083 V/cm
Time required	117 h	180 h	60 h
Cell potential	120 V	77 V	3.34 V
Current	4,045 A/electrode	52 A/electrode	2.95 mA
Current required	3.6×10^6 A	3.7×10^6A	-
Power required	44,000 MW	35,000 MW	9.86 mW
Energy required	5.0×10^7 kW h	5.1×10^7 kW h	0.59 W h
Water removed	1.50×10^{10} kg	1.50×10^{10} kg	0.39 kg
Energy requirement	3.3 W h/kg	3.4 W h/kg	1.52 W h/kg

Conclusions

The methods presented in this work illustrate the manner in which a constitutive equation relating the change in solids content with time and applied electric field can be used to perform an economic assessment of electrokinetic dewatering. The observation that the electric field controls both the maximum solids content achievable and the time required to reach it severely constrains the application of electrokinetic dewatering strategies to an entire CSA. The approach, however, may be feasible if implemented as part of a continuous or semi-batch plant process.

Acknowledgments

This work was supported by Mosaic Fertilizer LLC, Charlotte Brittain, program monitor. The assistance of Richard D. Grove (Engineering Superintendent, Mosaic Fertilizer LLC) and Prof. David Bloomquist (Department of Civil and Coastal Engineering, University of Florida) is greatly appreciated.

References

Aoki, S. and Kishimoto, K., 1990, "Application of BEM to galvanic corrosion and cathodic protection," in C. Brebbia (ed.), *Topics in Boundary Element Research: Electrical Engineering Applications*, Vol. 7, Springer-Verlag, Heidelberg, Germany, pp. 103-120.

Barnett, C., 2008, "Mine field," *Florida Trend: The Magazine of Florida Business*, May, pp. 84-90.

Brebbia, C.A. and Walker, S., 1980, *Boundary Element Techniques in Engineering*, Butterworths & Co. Ltd., London.

Carrier, W.D., 2001, "Rapid clay dewatering phase II: field-scale tests," Technical report, Florida Institute of Phosphate Research.

Fourie, A.B., Johns, D.G. and Jones, C.J.F.P., 2007, "Dewatering of mine tailings using electrokinetic geosynthetics," *Can. Geotech. J.*, Vol. 44, pp. 160-172.

Gray, L. and Paulino, G., 1997, "Symmetric Galerkin boundary integral formulation for interface and multi-zone problems," *International Journal for Numerical Methods in Engineering*, Vol. 40, pp. 3085-3101.

Hartmann, F., Katz, C. and Protopsaltis, B., 1985, "Boundary elements and symmetry," *Ingenieur Archiv*, Vol. 55, No. 6, pp. 440-449.

Ho, M.Y. and Chen, G., 2001, "Enhanced electro-osmotic dewatering of fine particle suspension using a rotating anode," *Industr. Eng. Chem. Res.*, Vol. 40, pp. 1859-1863.

McKinney, J.P., 2010, *Design of Electrolytic Dewatering Systems for Phosphatic Clay Suspensions*, PhD thesis, University of Florida.

McKinney, J.P. and Orazem, M.E., 2011, "A constitutive relationship for electrokinetic dewatering of phosphatic clay slurries," *Miner. Metall. Process.*, Vol. 28, No. 1, pp. 49-54.

McKinney, J.P., Orazem, M.E., Moghissi, O. and D'Zurko, D., 2006, "Development of ECDA criteria for prioritization of indications," *Proceedings of Corrosion/2006*, National Association of Corrosion Engineers, Houston, Texas, Paper 06-188.

Moghissi, O., McKinney, J.P., Orazem, M.E. and D'Zurko, D., 2009, "Predicting coating holiday size using ECDA survey data," *Proceedings of Corrosion/2009*, National Association of Corrosion Engineers, Houston, Texas, Paper 09-146.

Riemer, D.P., 2000, *Modeling Cathodic Protection for Pipeline Networks*, PhD thesis, University of Florida, Gainesville, Florida.

Riemer, D.P. and Orazem, M.E., 2000, "Application of boundary element models to predict effectiveness of coupons for assessing cathodic protection of buried structures," *Corrosion*, Vol. 56, No. 8, pp. 794-800.

Riemer, D.P. and Orazem, M.E., 2005a, "A mathematical model for the cathodic protection of tank bottoms," *Corros. Sci.*, Vol. 47, No. 3, pp. 849-868.

Riemer, D.P. and Orazem, M.E., 2005b, "Modeling coating flaws with non-linear polarization curves for long pipelines," in R.A. Adey (ed.), *Corrosion and Boundary Element Methods*, Vol. 12 of Advances in Boundary Elements, WIT Press, Southampton, UK, pp. 225-259.

Shang, J.Q. and Lo, K.Y., 1997, "Electrokinetic dewatering of a phosphate clay," *J. Hazard. Mater.*, Vol. 55, pp. 117-133.

Stakgold, I., 1979, *Greens Functions and Boundary Value Problems*, John Wiley & Sons, New York.

Telles, J., Wrobel, L., Mansur, W. and Azevedo, J., 1985, "Boundary elements for cathodic protection problems," in C.A. Brebbia and G. Maier (eds), *Boundary Elements VII*, Vol. 1, Springer-Verlag, Heidelberg, pp. 63-71.